REPORT DOCUMENTATION PAGE

AFRL-SR-AR-TR-04-

0063

1. REPORT DATE (DD-MM-YYYY)	2. REPORT TYPE	6/1/01-11/30/03
January 2, 2004	Final Performance Report	

4. TITLE AND SUBTITLE
Ion Dynamics Related to Hypersonics

5a. CONTRACT NUMBER
F49620-01-1-0430

5b. GRANT NUMBER

5c. PROGRAM ELEMENT NUMBER

6. AUTHOR(S)
Shuji Kato, Veronica M. Bierbaum, and Stephen R. Leone

5d. PROJECT NUMBER

5e. TASK NUMBER

5f. WORK UNIT NUMBER

7. PERFORMING ORGANIZATION NAME(S) AND ADDRESS(ES)

The Regents of the University
of Colorado

572 UCB
Boulder, CO 80309-0572

8. PERFORMING ORGANIZATION REPORT NUMBER

9. SPONSORING / MONITORING AGENCY NAME(S) AND ADDRESS(ES)

Dr. Michael R. Berman
AFOSR/NL
4015 Wilson Boulevard, Rm 713
Arlington, VA 22203-1954

10. SPONSOR/MONITOR'S ACRONYM(S)

11. SPONSOR/MONITOR'S REPORT NUMBER(S)

12. DISTRIBUTION / AVAILABILITY STATEMENT

Approved for Public Release; distribution is unlimited.

20040203 016

13. SUPPLEMENTARY NOTES

14. ABSTRACT
This research focused on the study of reactivity and dynamics of ion systems with relevance to atmospheric chemistry and combustion processes. The mobility of the fuel ion, $t\text{-}C_4H_9^+$, was measured drifting in polar and nonpolar atmospheric gases. These measurements were compared to polarization theory and locked dipole estimates as well as to related ion mobility measurements to better understand differences in interaction potentials. Unimolecular and bimolecular reactions of the $t\text{-}C_4H_9^+$ ion, among other hydrocarbon ions, were also studied to elucidate the stability and reactivity in combustion. The study was also extended to gas phase chemistry of deprotonated nitroalkane anions ($R_2C{=}NO_2^-$), key intermediates in ion-enhanced combustion/detonation of nitroalkanes. A technique to detect and quantify the neutral radical products of ion reactions was developed and improved. The results are especially relevant to fuel ion-molecule reactions and transport properties important in reducing ignition delay time and improving efficiency in hypersonics.

15. SUBJECT TERMS
Atmospheric reactions, Ion-molecule interactions, Transport properties, Ion mobility, Fuel combustion, Ignition delay time, Selected ion flow tube

16. SECURITY CLASSIFICATION OF:			17. LIMITATION OF ABSTRACT	18. NUMBER OF PAGES	19a. NAME OF RESPONSIBLE PERSON
a. REPORT	b. ABSTRACT	c. THIS PAGE			Veronica M. Bierbaum
Unclassified	Unclassified	Unclassified	Unclassified Unlimited	5	19b. TELEPHONE NUMBER (include area code) 303-492-7081

"Ion Dynamics Related to Hypersonics"

AFOSR Grant F49620-01-1-0430

(Grant Period: 1 June 2001 – 30 November 2003)

Final Performance Report - 2 January 2004

Stephen R. Leone and Veronica M. Bierbaum - Principal Investigators
JILA and the Department of Chemistry and Biochemistry
University of Colorado
Boulder, Colorado 80309-0440
Department of Chemistry, Department of Physics, and Lawrence Berkeley National Laboratory
University of California, Berkeley
Berkeley, CA 94720

Executive Summary

The goal of this research is to study the transport properties and chemical reactions of atmospheric ions and hydrocarbon fuel ions that are relevant to issues of hypersonic flight, in particular to the enhanced ignition and combustion of aviation fuels. Experiments focus on the measurements of mobilities and reactivities of fuel ions in a variety of gaseous media using flow drift and selected ion flow tube (SIFT) techniques. Specifically, the tertiary butyl cation t-$C_4H_9^+$ is extensively investigated due to its high yield and nonreactive characteristics in typical hydrocarbon combustion and ion-enhanced combustion processes.

The mobility of t-$C_4H_9^+$ drifting in He, N_2, O_2, and H_2O is measured and compared to theoretical calculations and similar ion mobility measurements. The reduced zero-field mobilities of t-$C_4H_9^+$ in He, N_2, O_2, and H_2O are determined to be $K_0^{(0)} = 14.8 \pm 0.6$, 3.7 ± 0.8, 3.3 ± 0.8, and 0.04 ± 0.02 $cm^2\ V^{-1}\ s^{-1}$, respectively. While the mobility values in the nonpolar gases are in general agreement with theoretical calculations, the mobility in H_2O is extraordinarily low. Collision-induced dissociation of t-$C_4H_9^+$ indicates that the ion is stable with the dissociation threshold energy (E_{cm}) of approximately 2 eV. Compared to other hydrocarbon cations, the t-$C_4H_9^+$ ion is totally non-reactive with O_2, N_2O, NO, and NO_2 (reaction rate coefficient $k < 10^{-12}$ $cm^3\ s^{-1}$) in a drift field of up to $E/N \approx 60$ Td ($E_{cm} \approx 0.7$ eV).

The SIFT study has also been extended to gas phase chemistry of deprotonated nitroalkane anions ($R_2C{=}NO_2^-$), key intermediates in ion-enhanced combustion/detonation of nitroalkanes. A VUV laser-ionization time-of-flight mass spectrometry to detect and quantify

the neutral radical products of air plasma ion reactions, specifically methyl radical, has been developed and a higher detection sensitivity achieved. These results are essential for the comprehensive understanding and modeling of plasma and combustion processes.

Professional Personnel Associated with the Research

Co-principal Investigators

Stephen R. Leone

Veronica M. Bierbaum

Senior Research Associate

Shuji Kato

Post-doctoral Research Associates

John Husband

Graduate Research Associates

Louis Haber

Publications

S. R. Leone, J. Husband and V. M. Bierbaum, *Mobility determinations of molecular ions for hypersonics*, American Institute of Aeronautics and Astronautics, **2003 – 705**, 1 (2003).

J. Husband and S. R. Leone, "Mobilities: Small Systems", *The Encyclopedia of Mass Spectrometry, Volume 1. Theory and Ion Chemistry*, Edited by M. L. Gross and R. Caprioli, Elsevier, Amsterdam, 2003, p. 498.

S. Kato, S. R. Leone, V. M. Bierbaum and L. H. Haber, *Mobilities and reactivities of molecular ions in combustion and hypersonics*, American Institute of Aeronautics and Astronautics, **2004 – 1015**, 1 (2004).

L. H. Haber, J. Husband, J. Plenge and S. R. Leone, *Mobility of t-$C_4H_9^+$ in polar and nonpolar atmospheric gases*, Chemical Physics Letters (in press).

S. Kato, K. E. Carrigan, C. H. DePuy and V. M. Bierbaum, *Gas phase ion-molecule reactions of small nitroalkanes and their deprotonated anions*, European Journal of Mass Spectrometry (in press).

Interactions/Transitions

Discussions with Al Viggiano, Skip Williams, Rainer Dressler and Ed Murad of the Air Force Research Laboratory, concerning combustion ignition, the relevant ions that may be involved in enhancing ignition, their mobilities and reactive chemistry.
Participation in AIAA Symposia on 5th Weakly Ionized Gases Workshop, Reno, NV, January 2003 and 6th Weakly Ionized Gases Workshop, Reno, NV, January 2004.

New discoveries, inventions, or patent disclosures

None

Honors/Awards

S. R. Leone

Member - National Academy of Sciences
Fellow - American Physical Society
Fellow - Optical Society of America
Fellow - American Association for the Advancement of Science
Fellow - American Academy of Arts and Sciences
Centennial Lecturer of the American Physical Society

Introduction

Ion-enhanced combustion has attracted increasing research interest.[1,2] Small additions of certain compounds have been known to enhance the efficiency of combustion and ignition dramatically, presumably via assisting formation of free radicals that initiate chain reactions.[3,4] Analogously, injection of certain ions in fuels is expected to generate radicals through ion-molecule reactions and enhance the rate of combustion.[1,2] Once the initial radicals are formed, subsequent chain reactions are considered to proceed with little or no activation barriers. Computational modeling studies have shown that introducing greater ionization into the fuel plasma will reduce the ignition delay time and improve hydrocarbon combustion.[2]

Accurate models of ion-enhanced combustion or ignition will rely on a complete understanding of parameters such as reaction rates, dissociation pathways, and ion transport properties. Although the mobility, diffusion, and velocity distributions of ions in a drift field have been important areas of research for many years,[5] the mobility values for many simple

hydrocarbon cations remain unknown. It is especially so for fuel molecules that would occur in ion-injection ignition processes for hypersonic aircraft. Reaction rates and product branching ratios of hydrocarbon cations $C_nH_{2n+1}^+$ have recently been studied at room temperature;[2] however, reactivities at elevated temperatures or in a drift field are yet to be fully understood.

The mobilities, stabilities, and reactivities of hydrocarbon ions, such as t-$C_4H_9^+$ among several other alkyl cations, are the target of the present study. In atmospheric fuel combustion and ion-injection ignition, the $C_4H_9^+$ ion is particularly stable and is the major and terminal product of NO^+, O_2^+, O^+, N^+, and N_2^+ reacting with isooctane (iso-C_8H_{18}).[1] We thus focus on the transport property of t-$C_4H_9^+$ and study the mobility in various gases. The first measurements of $C_4H_9^+$ mobilities have recently been made with helium, N_2, and O_2.[6] In addition to the nonpolar gases, we newly measure the mobility of $C_4H_9^+$ in strongly polar H_2O gas.[7] Water vapor is itself an important constituent in combustion environments. The results are discussed in terms of polarization theory and locked dipole calculations as well as in comparison with earlier mobility measurements performed on aromatic ions[8] and many atmospheric cluster ions.[9-11]

During the above measurements, t-$C_4H_9^+$ ions are found to be extremely stable and unreactive. Although there are many reactions known for t-$C_4H_9^+$ ions including hydride transfer with large hydrocarbons,[12] remarkably few reactions have been reported with small molecules pertinent to atmospheric combustion. For example, t-$C_4H_9^+$ is unreactive with H_2O, N_2, O_2,[6] and even with ozone[2] in the absence of drift field at room temperature. Here, we study the reactivities of t-$C_4H_9^+$ ions with O_2, N_2O, NO, and NO_2 in a drift field over a wide range of electric field; the ions are translationally (and also possibly internally) excited and potentially react with these small molecules. We also explore the stability of t-$C_4H_9^+$ by collision-induced dissociation (CID). Early studies of unimolecular dissociation of t-$C_4H_9^+$ employed high collision energies (up to keV), and dissociation pathways and product structures have been controversial.[13-15] We conduct CID at low collision energies pertinent to plasma and combustion environments. These results are specifically relevant to ion-injection processes for efficient combustion in hypersonics.

The results in previous grant periods provide a strong basis for the above studies. Arrival time measurements were used to determine the mobilities of aromatic ions and several atmospheric cluster ions, while Doppler resolved laser-induced fluorescence was previously used to examine the velocity distributions and molecular alignment of ions in drift fields.

Comprehensive reaction studies of $N_2^+(v)$ yielded vibrational state-specific reaction rates for reactions with HCl, CO and NO as well as vibrational deactivation rates in collisions with N_2 and O_2. Vibrational product distributions from the reactions of O_2 with Ar^+ and Xe^+ were also measured. Initial experiments using VUV laser-ionization-time-of-flight (TOF) mass spectrometry succeeded in making the first detection of the methyl radical formed in the gas phase ion-molecule reactions of CO^+ with CH_4 and N_2O^+ with CH_4.[16] VUV generation was optimized in a four-wave mixing cell with xenon leading to a highly improved photoionization of nitric oxide. The present study further explores the VUV-ionization-TOF technique for improvement in the detection sensitivity. Pertinent to hydrocarbon ion-enhanced fuel combustion, deprotonated nitroalkane ions ($R_2C{=}NO_2^-$) have been known to be key intermediates in ion-enhanced combustion/detonation of nitroalkane fuels/explosives.[4,17,18] We thus investigate fundamental gas phase chemistry of a series of nitroalkane anions. These studies all work towards a better understanding of plasma and combustion processes.

Methods and Procedures

Selected Ion Flow-Drift Tube (SIFDT) apparatus

A selected ion flow-drift tube (SIFDT)[19] apparatus has been constructed and modified to make arrival time measurements, CID experiments, and reaction rate determinations with a focus on fuel molecules (Figure 1). In this apparatus, target ions are generated by selection of a suitable precursor gas undergoing electron impact in the flowing afterglow source. The ions then pass through a quadrupole mass filter and are injected into the drift tube. The drift section consists of stacked drift rings, each being 10 mm in width. Within the drift tube the selected ions are accelerated in a constant field through a neutral buffer gas, before passing through a sampling orifice at the entrance of a quadrupole mass spectrometer. Ions are detected with the electron multiplier (CDEM). The double quadrupole arrangement ensures that only ions of the desired mass are injected into the drift tube, and that the measured mobility can be correlated to these injected ions without interference from products of reactions occurring in the drift tube.

In the source region electron impact on helium buffer gas was used to make He metastables, which react with a suitable precursor gas added downstream of the ionizer. Neopentane was primarily used to generate hydrocarbon ions such as $C_4H_9^+$, $C_3H_5^+$, and $C_2H_5^+$ in high yields for mobility measurements (Figure 2). $C_4H_9^+$ ions were also generated from

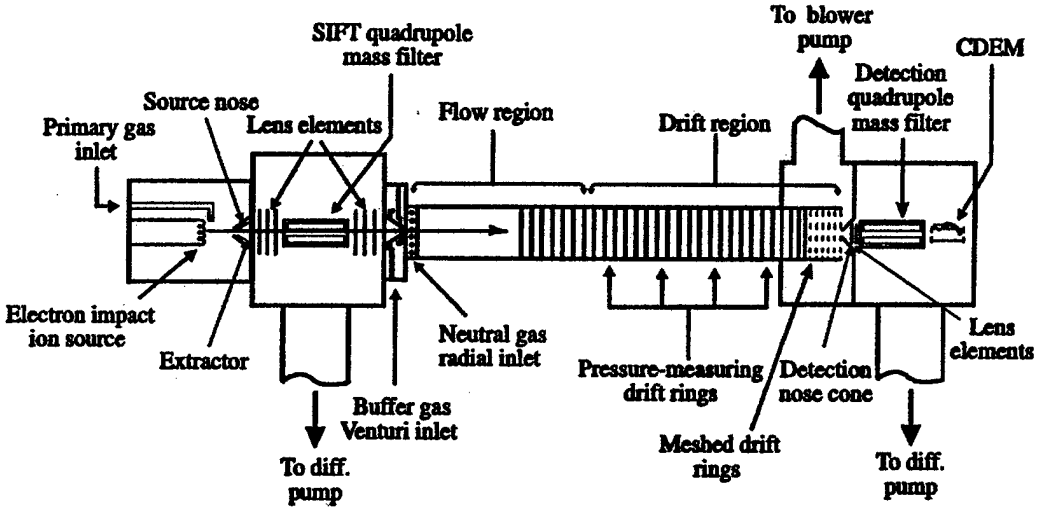

Figure 1: SIFDT apparatus. The SIFT injection orifice connects the SIFT quadrupole mass filter region and the flow/drift tube. The flow/drift tube section has attached multiple neutral inlets located along the tube. Ions are detected with the electron multiplier (CDEM).

different sources, e.g., electron impact on t-butyl chloride or dissociative proton transfer from H_3O^+ to t-butyl chloride or t-butanol. We found that the ion, $C_4H_9^+$, could be reproducibly created in high yield and with high selectivity by varying the electron impact settings such as voltage, current and seed gas pressure (Figure 2a), enabling the alteration of the experimental system towards a simpler, more efficient drift tube configuration with the ion source inside the flow tube, thus bypassing the need for the SIFT. Using this slightly altered drift-tube system, the mobility of $C_4H_9^+$ was investigated drifting in He, N_2, O_2, and H_2O, resulting in successful and consistent measurements.

The SIFT-drift apparatus was disassembled prior to the Leone group's move to the University of California at Berkeley. All parts were cleaned and several minor alterations were made to improve the overall performance of the instrument. Finally, the apparatus was successfully reassembled and used for continuing ion mobility measurements.

Mobility measurements

The ions of interest were entrained in a helium buffer flow typically at 0.4 Torr and 300 K. For mobility measurements in a gas mixture, N_2, O_2, or H_2O was added to the helium flow prior to the drift section. A sample source for introducing well-regulated flows of water vapor was designed and constructed for the present study; a reservoir of deionized water in the liquid

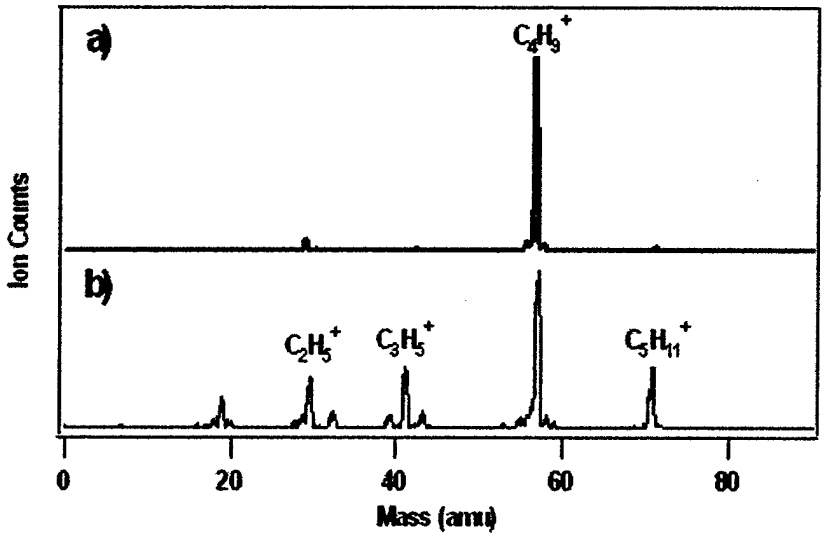

Figure 2: Mass spectra of hydrocarbon ions formed from neopentane after electron impact. (a) Source conditions optimized for $C_4H_9^+$ production. (b) Source conditions changed to generate other ions in addition to $C_4H_9^+$.

phase was attached to a line connected by a metering valve and flow meter, permitting a small, variable, and measured flow rate of water vapor into the flow tube. Lower pressures of H_2O were used to prevent formation of water clusters.

The ions can freely drift in a uniform electric field. Measurements were taken by recording arrival time scans at different applied drift fields. Arrival times were measured by a dual-pulse depletion technique;[6] two drift rings of a separation of 20 cm were simultaneously pulsed (+60 V, 40 μs wide) so as to drive ions axially away from the pulsed rings producing two minima in the otherwise constant ion signal (Figure 3). The two minima were detected with an electron multiplier coupled to a multi-channel scaler and the arrival time difference measured.

The drift velocity v_d (in cm s^{-1}) at a drift field E (in V cm^{-1}) is given by the difference between the ion velocity at the applied field and that at zero field. The mobility K (in cm^2 V^{-1} s^{-1}) is simply:

$$K = v_d / E \qquad (1)$$

To compare mobilities measured at different pressures (p in Torr) and temperatures (T in Kelvin), the reduced mobility, K_0, is usually quoted.

$$K_0 = \frac{p}{760} \cdot \frac{273.15}{T} \cdot K \qquad (2)$$

The field is usually quoted as E/N in units of Townsend, Td (1 Td = 10^{-17} V cm^2), where N is the number density of the gas (in cm^{-3}). In the present study, ion mobilities were determined in varied fields of up to $E/N \approx 30$ Td.

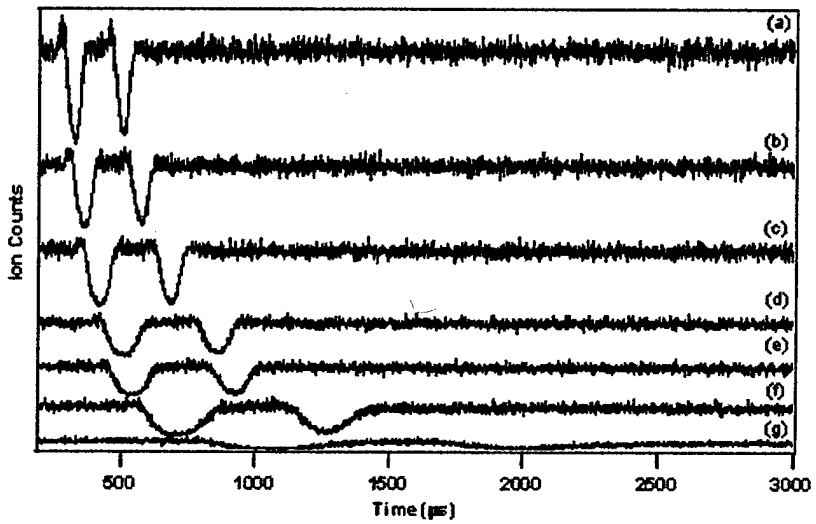

Figure 3: Arrival time measurements of $C_4H_9^+$ drifting in He at E/N of (a) 27.6 Td, (b) 22.0 Td, (c) 16.5 Td, (d) 11.0 Td, (e) 9.9 Td, (f) 5.5 Td, and (g) 2.2 Td.

Reactivity measurements

For reactivity studies, the flow/drift tube section has attached multiple neutral inlets located along the tube for reactivity studies. Hydrocarbon ions in a helium flow (≈ 0.5 Torr) were allowed to react with neutral reagents, O_2, N_2O, NO (5% in helium) or NO_2, added sequentially through the multiple inlets. This setup effectively changes the reaction time thereby allowing the kinetics of the parent ions to be followed and the ion-molecule reaction rates determined.[19] In order to attain high electric fields (up to $E/N \approx 60$ Td) and explore reactivities over a wide range of ion kinetic energies, higher drift voltages and reduced helium buffer pressures (0.3 - 0.4 Torr) were used. For the ion-molecule reactions of deprotonated nitroalkanes ($R_2C{=}NO_2^-$), the $[M\text{-}H]^-$ ions were generated by HO^- deprotonation of the corresponding neutral nitroalkanes $R_2HC\text{-}NO_2$ and similarly subjected to reactions with neutral reagents added downstream of the flow tube.

CID experiments were performed by injecting the t-$C_4H_9^+$ ions at varied injection energies (E_{lab} = 10 - 80 eV). Activation and dissociation of t-$C_4H_9^+$ takes place upon collision of

the ion with the helium buffer gas near the SIFT injection orifice (Figure 1). Both depletion of the parent ion and formation of products were monitored using the detection mass filter.

VUV-ionization-TOF mass spectrometry

The detection quadrupole mass filter (Figure 1) was replaced with a TOF mass spectrometer in this experimental setup. Reactant ions were produced in a flowing afterglow instrument, entrained in a stream of helium carrier gas, and then allowed to react with the neutral reactant introduced downstream. The radical products were selectively ionized by 10.5 eV (118 nm) light immediately before the sampling orifice (i.e., detection nose cone in Figure 1) of a time-of-flight mass spectrometer. Unreacted source ions and the product ions were excluded from the interaction region by applying a small voltage to a set of three grids located in the flow-tube in front of the laser beam entrance position. 118 nm light was generated by a four wave mixing process using the third harmonic (355 nm) of a Nd:YAG laser focused into a cell containing a mixture of xenon and argon. Detection of the methyl radical from $CO^+ + CH_4$ was used as a test case.

Results and Discussion

Mobilities of hydrocarbon ions

The mobility of t-$C_4H_9^+$ in pure helium (K_{He}) was measured first. Blanc's law[5] is used for mobility determination of an added buffer gas component (m = N_2, O_2, or H_2O):

$$1 / K_{mix} = \chi_{He} / K_{He} + \chi_m / K_m \qquad (3)$$

where K_{mix} is the mobility measured in the mixture and χ's are the mole fractions. For a given χ_m the reduced mobility is extrapolated to a zero drift field, and the results are shown in Figure 4 as a function of χ_m. The slope is significantly greater for H_2O (Figure 4b), clearly demonstrating that the mobility of t-$C_4H_9^+$ is very small in water vapor compared to those in N_2 and O_2.

For a given applied field, the slope of the Blanc's law plot similar to Figure 4 is used to derive the mobility for each buffer gas.[7] Results are shown in Figure 5 as a function of E/N. These data points are extrapolated to $E/N \rightarrow 0$ in order to obtain the reduced zero-field ion mobilities, $K_0^{(0)}$.

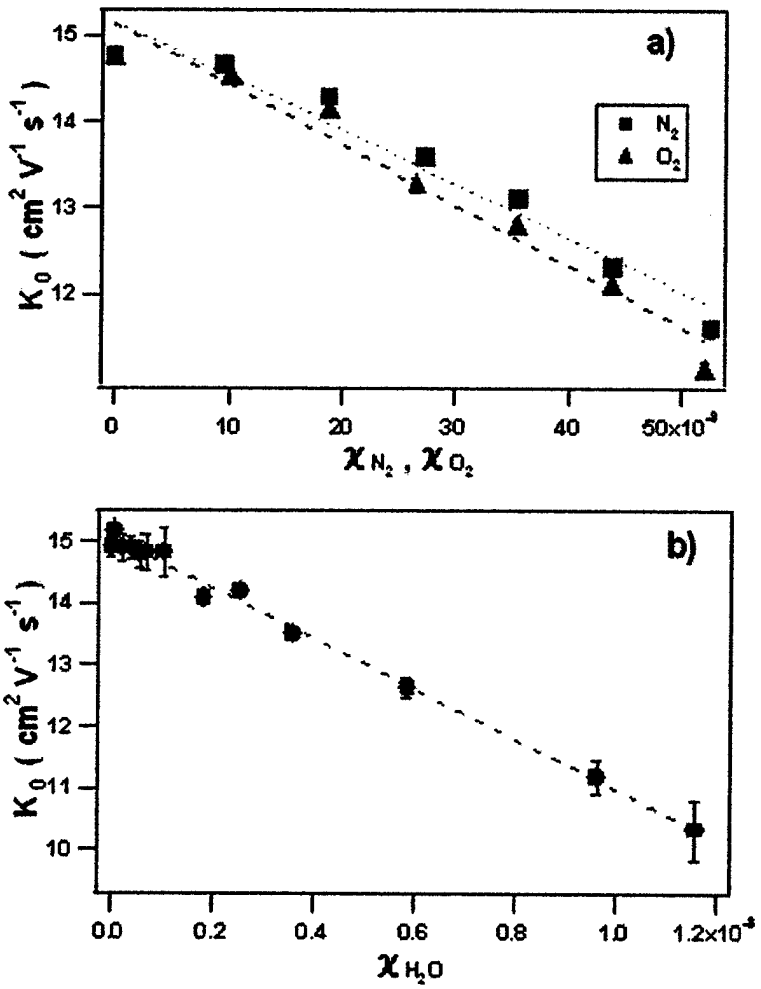

Figure 4: Mobility of t-$C_4H_9^+$ vs. mole fraction, χ, of the buffer gas in helium. (a) Addition of N_2 or O_2 up to ≈ 5 %. (b) Addition of H_2O up to ≈ 0.1 %.

The zero-field mobilities of t-$C_4H_9^+$ in He, N_2 and O_2 are determined to be 14.8 ± 0.6, 3.7 ± 0.8, and 3.3 ± 0.8 cm^2 V^{-1} s^{-1}, respectively (Figure 5a). The mobility of $C_4H_9^+$ is roughly equal in N_2 and O_2, due to similar sizes and interaction potentials, while the highest mobility is in He, which is smallest and has the weakest interaction potential. The value for helium is in good agreement with a previous measurement[6] and is slightly improved here. By comparison, the $C_4H_9^+$ ion is significantly less mobile in He than are smaller hydrocarbon cations commonly found in combustion, e.g., C^+ ($K_0^{(0)} = 21.8$ cm^2 V^{-1} s^{-1}), CH_2^+ (29.2), CH_4^+ (23.0), and CH_5^+ (21.0) in He at 300 K.[5] The mobility values are relatively constant in He, N_2 and O_2 over the range of *E/N* studied. This indicates that the ion-neutral interaction potential is dominated by

repulsive forces for these nonpolar buffer gases. The measured values are in general agreement with polarization mobilities, K_{pol},[5] of 17.6, 2.68 and 2.69 $cm^2\ V^{-1}\ s^{-1}$ for $C_4H_9^+$ drifting in He, N_2 and O_2, respectively,[7] calculated using the literature polarizability values.[20] As expected, mobilities are lower in the more polarizable gases, N_2 and O_2, than in He.

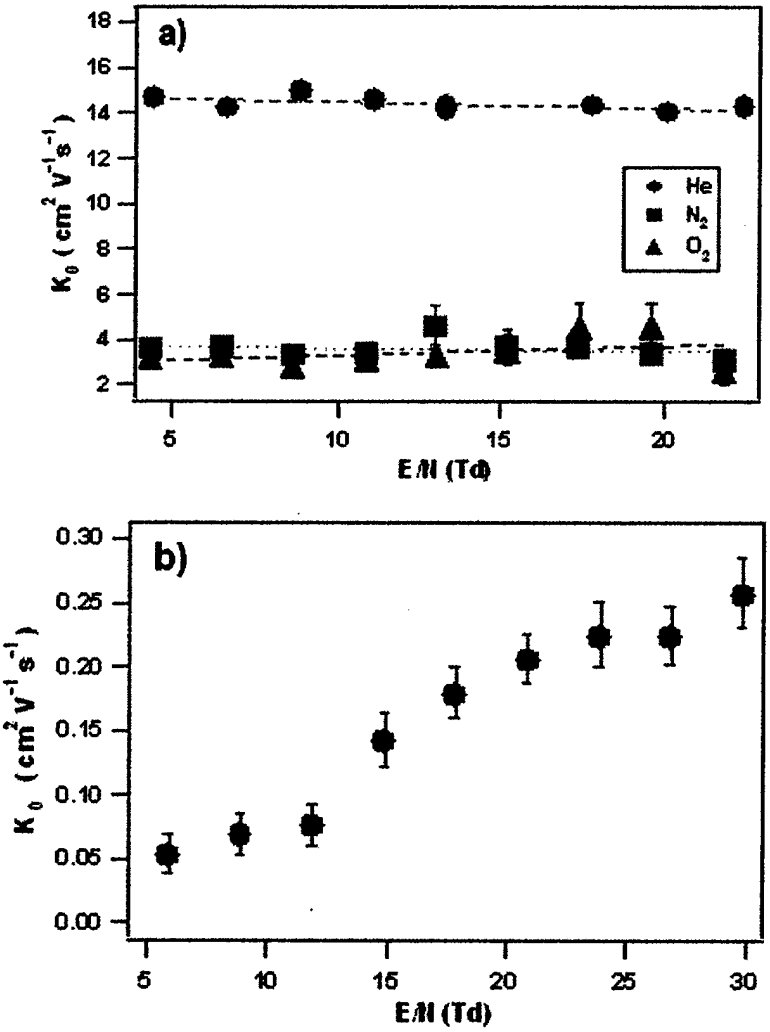

Figure 5: The ion mobilities of t-$C_4H_9^+$ drifting in (a) He, N_2, and O_2, and (b) H_2O, as a function of *E/N*.

The above theoretical model does not take into account factors such as the ion or molecule structure, energy transfer, internal degrees of freedom, and inelastic collisions. For example the experimental mobilities of $C_6H_6^+$ and $C_{12}H_{12}^+$ in He are 11.8 and 7.6 $cm^2\ V^{-1}\ s^{-1}$, respectively,[8] substantially smaller than the corresponding K_{pol} values of 17.4 and 17.1 $cm^2\ V^{-1}\ s^{-1}$. The experimental values are in better agreement with theoretical calculations that use the

angle-averaged hard sphere cross section method, which incorporates ion structure and predicts values of 11.4 and 7.6 $cm^2\ V^{-1}\ s^{-1}$, respectively.[8] The inclusion of ion structure will also be essential for more accurate calculations of the $C_4H_9^+$ mobility.

The mobility of t-$C_4H_9^+$ in H_2O is quite different in both the magnitude and trend (Figure 5b). The ion mobility is very small and decreases from 0.26 $cm^2\ V^{-1}\ s^{-1}$ (E/N = 29.8 Td) to 0.05 $cm^2\ V^{-1}\ s^{-1}$ (E/N = 6.0 Td). The strong dependence indicates that the interaction potential is dominated by attractive forces, as also observed in other strongly polar molecules.[10,11] The measured zero-field mobility of t-$C_4H_9^+$ in H_2O is 0.04 ± 0.02 $cm^2\ V^{-1}\ s^{-1}$. The small value is compared with other mobility values in water vapor, e.g., 0.66 and 0.43 $cm^2\ V^{-1}\ s^{-1}$ for NO^+ and $H_3O^+(H_2O)_3$, respectively.[11]

For highly polar H_2O, locked-dipole theory is used to calculate the $C_4H_9^+$ mobility (K_{ld}) as 0.68 $cm^2\ V^{-1}\ s^{-1}$,[7] using the polarizability and the permanent dipole moment for H_2O.[20] The value of K_{ld} is much closer to the experimental value than K_{pol} (3.44 $cm^2\ V^{-1}\ s^{-1}$); however, the discrepancy is still large. This indicates that a more complete theoretical model is needed for better description of the ion mobility and more accurate modeling of ion-enhanced hydrocarbon combustion processes.

CID and ion-molecule reactions of t-$C_4H_9^+$

Unimolecular and bimolecular reactivities of t-$C_4H_9^+$ were studied using the SIFDT apparatus specifically modified for this purpose. Dissociation of t-$C_4H_9^+$ is negligible upon collision with He at an injection energy E_{lab} of 10 eV (Figure 6a), whereas the ion fragments extensively at 35 eV (Figure 6b) and it is almost completely dissociated beyond 50 eV. Product species $C_3H_5^+$ and $C_2H_5^+$ are observed via losses of methane and ethylene, respectively (Figure 6b). These are the two lowest dissociation channels with the theoretical reaction enthalpies of 180 kJ mol^{-1} (eq 4a) and 246 kJ mol^{-1} (eq 4b).[15,21]

$$t\text{-}C_4H_9^+ \rightarrow C_3H_5^+ + CH_4 \qquad (4a)$$

$$\rightarrow C_2H_5^+ + C_2H_4 \qquad (4b)$$

Figure 7 shows the collision energy dependence of product distributions observed in the CID of t-$C_4H_9^+$. At higher E_{lab}, the $C_3H_5^+$ and $C_2H_5^+$ ions further fragment to $C_3H_3^+$ and $C_2H_3^+$, respectively. Dissociation via the higher energy channel (eq 4b) becomes the major pathway as

the collision energy is increased, in contrast to the CID result in the keV collision energy regime which observed the opposite trend.[14] Our low-energy results appear to be consistent with the theoretical energy diagram.[15,21]

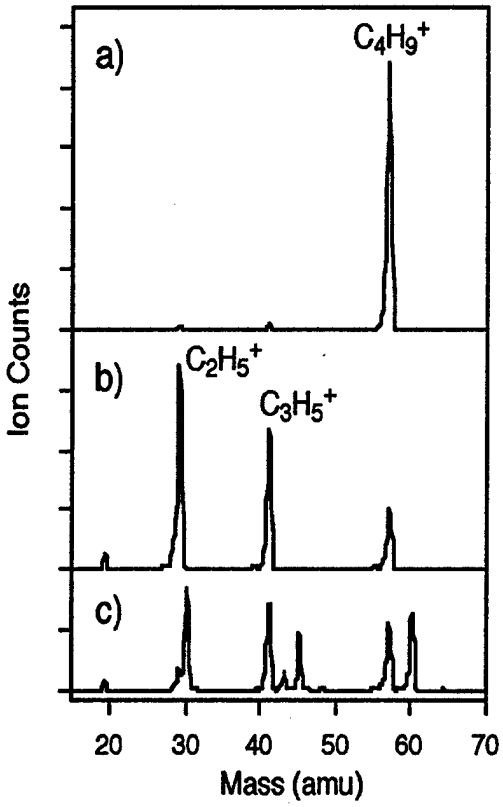

Figure 6: Mass spectra following SIFT injection of t-$C_4H_9^+$. (a) Injection energy E_{lab} = 10 eV. (b) Injection energy E_{lab} = 35 eV. (c) Injection at E_{lab} = 35 eV followed by addition of NO_2. All spectra are taken at 300 K with zero drift field.

Experimental determinations of dissociation threshold energies are relatively rare for hydrocarbon cations. It should be noted that under the present CID conditions, injected t-$C_4H_9^+$ ions undergo multiple collisions with high-pressure He. *Nominal* center-of-mass collision energies (E_{cm}) are computed from the relation $E_{cm} = E_{lab} \bullet m_{He}/(m_{He} + m_{ion})$, where m_{He} and m_{ion} are the masses of He and t-$C_4H_9^+$, respectively. One must be cautious with E_{cm} in the multiple collision regime and hence we quote the data as *nominal* E_{cm}. It is interesting to note, however, the qualitative agreement between the observed threshold E_{cm} and theoretical dissociation energy.[22] It is thus tempting to derive the threshold dissociation energy of t-$C_4H_9^+$ as approximately 2 eV ($\approx$ 190 kJ mol^{-1}), from the observed CID energy dependence and collision energy calibration routinely carried out in our laboratories using well-characterized standard

ions. The obtained threshold energy is qualitatively in line with the theoretical energy requirement for channel 4a ($\Delta_{rxn}H_{298}$ = 180 kJ mol^{-1}). Future experiments will measure the threshold energy under single collision conditions using the triple quadrupole capability that is accessible as one of our instrumental setups.

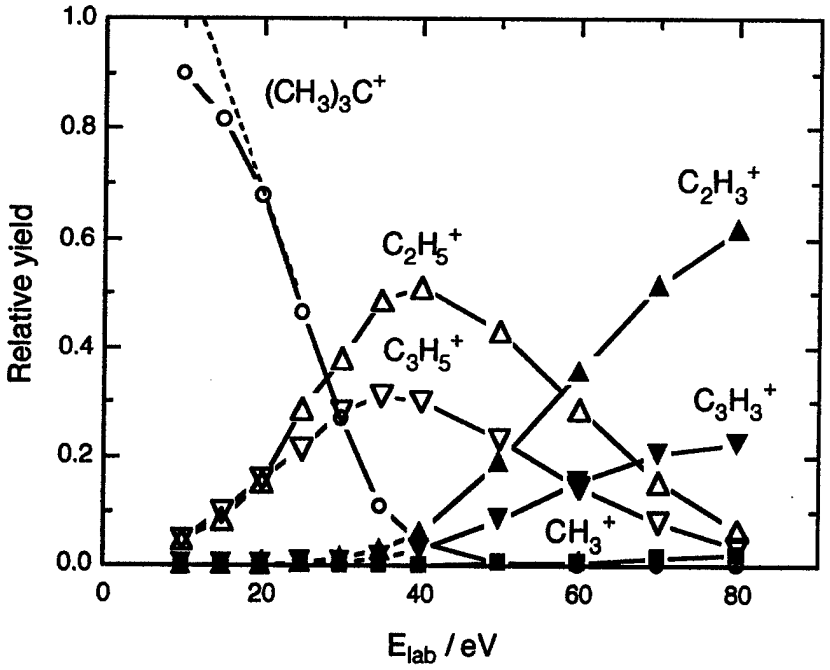

Figure 7: Product distributions from CID of the t-$C_4H_9^+$ ion [$(CH_3)_3C^+$]. Peak abundances have been normalized with respect to each other and are plotted against laboratory collision energy (E_{lab}). The broken line attached to the $(CH_3)_3C^+$ curve extrapolates to the nominal dissociation threshold at $E_{lab} \approx 12$ eV.

Ion-molecule reactions of t-$C_4H_9^+$ were examined with O_2, N_2O, NO, and NO_2. SIFT-injection of t-$C_4H_9^+$ at E_{lab} = 10 eV (Figure 6a) affords the ion in a very clean reaction environment free from other interfering ions or neutral precursors. O_2 is inherently a major component in the early stage of the fuel combustion process. N_2O supports combustion at elevated temperatures, and NO and NO_2 are reactive radicals commonly referred to as NO_x being produced in combustion. NO_2 is a strong oxidizer and is itself a homogeneous catalytic additive that assists the oxidation and spontaneous ignition of hydrocarbons.[3] A recent study showed that t-$C_4H_9^+$ does not react with O_2 or O_3 at 300 K even though there are product channels available with exothermicities of nearly 300 kJ mol^{-1}.[2] Our present results also indicate that t-$C_4H_9^+$ is

non-reactive with O_2, N_2O, NO, and NO_2 at 300 K ($k < 10^{-12}$ cm^3 s^{-1}). Figure 6c shows the result with NO_2. No change in the t-$C_4H_9^+$ signal intensity is observed over a wide range of added NO_2 ($\leq 6 \times 10^{13}$ cm^{-3}) while the CID products $C_2H_5^+$ and $C_3H_5^+$ both react with NO_2 moderately fast. A similar result is obtained in the reaction with NO.

The above reactions were then examined in a drift field. The center-of-mass collision energy of an ion-neutral pair in a buffer gas is given by

$$E_{cm} = \frac{m_r(m_i + m_b)}{2(m_i + m_r)} v_d^2 + \frac{3}{2} k_B T = \frac{3}{2} k_B T_{eff} \qquad (5)$$

where m_i, m_r, and m_b are ion, reactant, and buffer gas masses, respectively, and v_d is the ion drift velocity derived using the relationship in eqs 1 and 2. T_{eff} is the effective temperature upon collision of the ion and reactant. Because t-$C_4H_9^+$ is a large polyatomic species with many low-frequency vibrational modes, it can acquire internal excitation by collisions with the buffer gas helium through transit in the drift field. Therefore, the effective temperature as derived from eq 5 is likely to be a lower limit in this case.

Reagent gases O_2, N_2O, NO, or NO_2 were added to the reaction flow tube in amounts that are sufficiently small (< 1% of helium buffer gas) to not alter the ion mobility significantly (Figure 4a) and yet large enough to observe slow ion-molecule reactions. Drift fields of 0 - 60 Td were applied over a long reaction distance of 65 cm. The field corresponds to E_{cm} of 0.04 - 0.7 eV and T_{eff} of 300 - 5000 K for collisions of t-$C_4H_9^+$ with O_2, N_2O, NO, or NO_2. The range of T_{eff} covers well the temperatures relevant to plasma and combustion chemistry. In spite of the translational (and also possibly internal) excitation, no reaction is observed within the detection limits ($k < 10^{-12}$ cm^3 s^{-1}) between t-$C_4H_9^+$ and the added reagents, even with the more reactive radical species NO and NO_2. This suggests that the butyl cation may indeed be the most stable t-$C_4H_9^+$ structure and not sec-$C_4H_9^+$, which exhibits reactivities with several reagents.[2] It is noted that no unimolecular decomposition is observed for t-$C_4H_9^+$ in the drift field, which is reasonable in view of the relatively high dissociation threshold measured here (~ 2 eV). These results demonstrate the extremely high stability and low chemical reactivity of t-$C_4H_9^+$ as a major terminal ion in the fuel combustion process. Reactivity studies with more reactive O atoms have been proposed.[2]

Reactivities of nitroalkane anions

The above results are specifically relevant to ion-injection processes for combustion in hypersonics. Reactions of air plasma cations with fuel alkanes generate reactive radicals which propagate the chain reaction thereby reducing ignition delay time and improving combustion efficiency.[1,2] A similar mechanism involving deprotonated anions of nitroalkanes ($R_2C{=}NO_2^-$, or "*aci*-anion") has been proposed for the early stage of ion-sensitized combustion/detonation of nitroalkane propellants and explosives in the condensed phase.[4,17,18] We extended our study to the gas phase chemistry of *aci*-anions of several nitroalkane propellants, i.e., nitromethane, nitroethane, 2-nitropropane, 2-methyl-2-nitropropane, and nitrocyclopropane,[23] with the aim of providing complementary information about the intrinsic stability and reactivity of these ions. We found that these nitroalkane *aci*-anions exhibit specific S_N2 (nucleophilic substitution) reactions with CH_3I and chemical reactivities with CO_2, CS_2, and SO_2;[23] however, in the gas phase at 300 K, reactions of these ions with the parent nitroalkane molecules do not generate anionic species ($RNO_2^{-\bullet}$) which are considered pertinent to ion-sensitized combustion/detonation. Future studies will include reactions at high kinetic energies in a drift field. Such a study will provide an integrated view and understanding of a variety of ion-enhanced processes related to combustion and detonation.

Sensitivity improvements in radical detection

The detection sensitivity in VUV-TOF mass spectrometry was increased by several means, e.g., improving the VUV generation and photo-ion detection efficiencies and removing residual light which is a source of the background signals. First, VUV generation was markedly improved by using a phase matched mixture of xenon in argon and by purifying the mixture by circulating the contents of the cell through a dry ice/ethanol cold trap. The 118 nm generation as measured by the photoionization of nitric oxide was increased by an order of magnitude after these changes. The detection efficiency of the photo-ions was significantly improved when a modest acceleration field was created in the interaction region. This field serves to draw photo-ions into the detection region. Results for the photoionization of nitric oxide show a smooth increase in signal levels as the field strength increases up to ~30 V cm^{-1}. For the radical product studies the field strength was kept low (< 5 V cm^{-1}) to prevent possible interferences from electron impact or collision-induced dissociation of species accelerated in the field. With these

changes in effect, signal levels for the methyl radical were significantly improved over those previously reported from this project.

To both identify *and* quantify radical products from more complicated ion-molecule reactions, we modified the existing instrument to prevent residual 355 nm light entering the chamber. Removal of the 355 nm beam will enable us to unambiguously assign photo-ion signal as arising from single photon ionization of neutral species at 118 nm. To achieve this aim a rotatable lithium fluoride prism was mounted at the exit of the tripling cell. Rotating this prism allows the 118 nm beam to enter the chamber while the 355 nm beam strikes a beam block. Photoelectrons ejected from a Pt disc located at the laser exit of the chamber register the presence of the 118 nm beam. With this setup we observed the photoionization of nitric oxide at 118 nm with the 355 nm beam blocked from entering the chamber. The next step in this program is to further increase photo-ion detection efficiency to compensate for the much lowered 118 nm light intensity arising from the striking the lithium fluoride prism at a grazing angle. To this end the instrument will be modified to allow laser ionization behind the sampling orifice, between the acceleration plates of the time-of-flight mass spectrometer. This setup will provide essentially 100% detection of photo-ions.

Conclusion

The mobility of t-$C_4H_9^+$ drifting in He, N_2, O_2, and H_2O has been measured and compared to theoretical calculations and similar ion mobility measurements. t-$C_4H_9^+$ ion is significantly less mobile in He than are smaller hydrocarbon cations commonly found in combustion. The reduced zero-field mobilities in He, N_2, O_2 are in general agreement with calculated polarization mobilities, K_{pol}, and the inclusion of ion structure will be essential for more accurate predictions of the mobility. The mobility of t-$C_4H_9^+$ in H_2O is extraordinarily low. For highly polar H_2O, locked-dipole theory has been used to calculate the $C_4H_9^+$ mobility (K_{ld}). The value of K_{ld} is much closer to the experimental value than K_{pol} but the discrepancy is still large. A more complete theoretical model is needed for better description of the ion mobility and more accurate modeling of ion-enhanced hydrocarbon combustion processes.

Collision-induced dissociation experiments indicate that the t-$C_4H_9^+$ ion is very stable. The ion is totally non-reactive with small molecules pertinent to atmospheric combustion, O_2, N_2O, NO, and NO_2, in a drift field. These results demonstrate the extremely high stability and

low chemical reactivity of t-$C_4H_9^+$ as a major terminal ion in the fuel combustion process. Ion-molecule studies of deprotonated nitroalkane anions ($R_2C{=}NO_2^-$) have provided complementary gas-phase information about the properties of these species pertinent to ion-sensitized combustion/detonation of nitroalkanes in the condensed phase. A significant sensitivity improvement has been achieved for the VUV-TOF mass spectrometry applied to detection of atmospheric and combustion radicals.

These results can be used towards a greater understanding of the dynamics of ions in gases, especially regarding combustion and ignition. The ion and buffer gases studied in these experiments are specifically involved in hydrocarbon combustion and ignition processes under normal conditions. Ion transport properties and chemical reactivities are important parameters necessary for more accurate modeling in the pursuit of decreased ignition delay time and increased combustion efficiency in hypersonics.

References

1. S. T. Arnold, A. A. Viggiano, and R. A. Morris, J. Phys. Chem. A **101**, 9351 (1997).
2. S. Williams, T. M. Miller, W. B. Knighton, A. J. Midey, S. T. Arnold, A. A. Viggiano, and C. D. Carter, AIAA **2003-704**, 1 (2003).
3. V. Y. Shtern, The Gas-Phase Oxidation of Hydrocarbons (MacMillan, New York, 1964).
4. R. Engelke, W. L. Earl, and C. M. Rohlfing, Int. J. Chem. Kinet. **18**, 1205 (1986).
5. E. A. Mason and E. W. McDaniel, Transport Properties of Ions in Gases (Wiley, New York, 1988). H. W. Ellis, R. Y. Pai, E. W. McDaniel, E. A. Mason, and L. A. Viehland, Atom. Data Nucl. Data Tables **17**, 177 (1976). H. W. Ellis, M. G. Thackston, E. W. McDaniel, and E. A. Mason, Atom. Data Nucl. Data Tables **31**, 113 (1984).
6. S. R. Leone, J. Husband, and V. M. Bierbaum, AIAA **2003-705**, 1 (2003).
7. L. H. Haber, J. Husband, J. Plenge, and S. R. Leone, Chem. Phys. Lett. (in press).
8. M. Krishnamurthy, J. A. de Gouw, V. M. Bierbaum, and S. R. Leone, J. Phys. Chem. **100**, 14908 (1996).
9. M. Krishnamurthy, J. A. de Gouw, L. N. Ding, V. M. Bierbaum, and S. R. Leone, J. Chem. Phys. **106**, 530 (1996).

10. J. A. de Gouw, L. N. Ding, M. Krishnamurthy, H. S. Lee, E. B. Anthony, V. M. Bierbaum, and S. R. Leone, J. Chem. Phys. **105**, 10398 (1996).
11. J. A. de Gouw, M. Krishnamurthy, and S. R. Leone, J. Chem. Phys. **106**, 5937 (1997).
12. Y. Ikezoe, S. Matsuoka, M. Takebe, and A. A. Viggiano, Gas Phase Ion-Molecule Reaction Rate Constants Through 1986 (Maruzen, Tokyo, 1987).
13. A. Maquestiau, R. Flammang, and P. Meyrant, Int. J. Mass Spectrom. Ion Phys. **44**, 267 (1982).
14. S. A. McLuckey, C. E. D. Ouwerkerk, A. J. H. Boerboom, and P. G. Kistemaker, Int. J. Mass Spectrom. Ion Processes **59**, 85 (1984).
15. C. Aubry and J. L. Holmes, J. Phys. Chem. A **102**, 6441 (1998).
16. J. Li, V. M. Bierbaum, and S. R. Leone, Chem. Phys. Lett. **313**, 76 (1999).
17. Y. A. Gruzdkov and Y. M. Gupta, J. Phys. Chem. A **102**, 2322 (1998).
18. E. Woods III, Y. Dessiaterik, R. E. Miller and T. Baer, J. Phys. Chem. A **105**, 8273 (2001).
19. J. M. Van Doren, S. E. Barlow, C. H. DePuy and V. M. Bierbaum, Int. J. Mass Spectrom. Ion Processes **81**, 85 (1987).
20. Handbook of Chemistry and Physics (D. R. Lide, ed., CRC Press, Boca Raton, FL, 1993).
21. S. Sieber, P. Buzek, P. v. R. Schleyer, W. Koch, and J. W. de M. Carneiro, J. Am. Chem. Soc. **113**, 259 (1993).
22. S. J. Blanksby, S. Kato, V. M. Bierbaum, and G. B. Ellison, Aust. J. Chem. **56**, 459 (2003).
23. S. Kato, K. E. Carrigan, C. H. DePuy, and V. M. Bierbaum, Eur. J. Mass Spectrom. (in press).